Two-Dimensional Fourier Transform Raman Correlation Spectroscopy Study of Composition-Induced Structural Changes in a Series of Ethylene/Vinyl Acetate Copolymers

Yanzhi Ren,[†] Masahiko Shimoyama,[‡] Toshio Ninomiya,[‡] Kimihiro Matsukawa,[§] Hiroshi Inoue,[§] Isao Noda,*[,||] and Yukihiro Ozaki*[,†]

Department of Chemistry, School of Science, Kwansei Gakuin University, Nishinomiya 662-8501, Japan, Forensic Science Laboratory, Hyogo Prefectural Police Headquarters, Shimoyamate-dori, Chuo-ku, Kobe 650-0011, Japan, Plastics Department, Osaka Municipal Technical Research Institute, Morinomiya, Joto-ku, Osaka 536-0025, Japan, and The Procter and Gamble Company, Miami Valley Laboratories, P.O. Box 538707, Cincinnati, Ohio 45253-8707

Received: March 15, 1999

Generalized two-dimensional (2D) FT-Raman correlation spectroscopy has been applied to the study of the composition-induced structural changes in eleven different ethylene/vinyl acetate (EVA) copolymers with vinyl acetate (VA) content varying from 6 to 42 wt %. The eleven copolymer samples have been divided into four sets according to their composition range, and 2D correlation analysis has been applied to detect the characteristic bands for each set. Throughout the composition range of EVA copolymers, the increase of VA content always causes the crystalline lamellae to shrink, the amorphous interlamellar layers to expand, the *all-trans* $-(CH_2)-_n$ conformers to decrease, and the gauche conformers to increase in population. In particular, for the EVA with 7 wt % VA, small addition of VA comonomers acts as spacers between adjacent methylene segments and converts the orthorhombic unit cell to the anisotropic unit cell, manifested by the correlation splittings at (1438 cm^{-1}, 1415 cm^{-1}) and (1446 cm^{-1}, 1434 cm^{-1}), respectively. For the EVA with 26 wt % VA, small addition of VA comonomers mainly shortens the length of continual methylene segments and shifts the orthorhombic band from 1415 to 1419 cm^{-1}. The 2D correlation analysis has identified the cause-effect relationship for structural events occurring both at the supermolecular phase scale and at the segmental submolecular level.

Introduction

Generalized two-dimensional (2D) correlation spectroscopy,[1] which is an extension of the original 2D correlation spectroscopy proposed by Noda in 1986,[2−4] has received great attention in recent years. This novel 2D correlation method can be applied to the analysis of spectral signals which change as functions of not only time but also any other kinds of reasonable physical variables, such as temperature, pressure, concentration, and composition. Generalized 2D correlation spectra emphasize spectral features not readily observable in conventional one-dimensional spectra. It can also probe the specific order of certain spectral events taking place with the development of a controlling physical variable. The type of spectral signals analyzed by the newly proposed 2D correlation method becomes virtually limitless, ranging from IR and Raman spectroscopy to X-ray and fluorescence spectroscopy.

Many applications of generalized 2D correlation spectroscopy have been reported,[5−19] including temperature-dependent spectral variations,[10−15] concentration-dependent spectral changes,[16,17] and 2D IR and Raman heterospectral correlation analysis,[18] as well as 2D near-infrared (NIR) and mid-infrared heterospectral correlation analysis.[19] In our previous paper we demonstrated the potential of 2D NIR-excited Fourier transform (FT) Raman correlation spectroscopy in a study of the miscibility of polymer blends.[20] In this paper we present a 2D FT-Raman study of the structural evolution in random copolymers with major commercial interest: EVA.

Raman spectroscopic studies of polymers have recently been revitalized with the introduction of NIR-excited FT-Raman and multichannel spectroscopy.[21−23] In the past it was often difficult to measure Raman spectra from material samples of practical importance, such as blends, degraded specimens, and heat treated samples, since fluorescence from these specimens was very intense. The specimen had to be carefully selected or purified. The advantage of NIR excitation is that fluorescence from a polymer sample is minimized. With the advent of NIR-excited FT-Raman spectroscopy, almost all kinds of polymer samples can be subjected to Raman measurements. The Raman technique also enables us to measure the vibrational spectra of real-world polymer samples, including those in the form of pellets.

2D correlation-assisted FT-Raman spectroscopy is used to explore the supramolecular, molecular, and submolecular events occurring in a series of ethylene/vinyl acetate (EVA) copolymers with the increase of vinyl acetate (VA) content. EVA is a commonly used copolymer especially as a major ingredient for adhesives. It is well-known that changes in the VA content cause variations in the physical properties such as crystallinity and impact strength.[24−26] Recently, we studied the VA content in EVA using FT-Raman spectroscopy and chemometrics.[27] Key spectral features of twelve different EVA copolymers with VA content varying in the 7−44 wt % range were unambiguously

* To whom correspondence should be addressed. Mailing address: School of Science, Kwansei Gakuin University, Nishinomiya 662-8501, Japan. Fax: +81-798-51-0914. E-mail: ozaki@kwansei.ac.jp.
[†] Kwansei-Gakuin University.
[‡] Hyogo Prefectural Police Headquarters.
[§] Osaka Municipal Technical Research Institute.
[||] The Procter and Gamble Co.

10.1021/jp990893l CCC: $18.00
Published on Web 07/21/1999

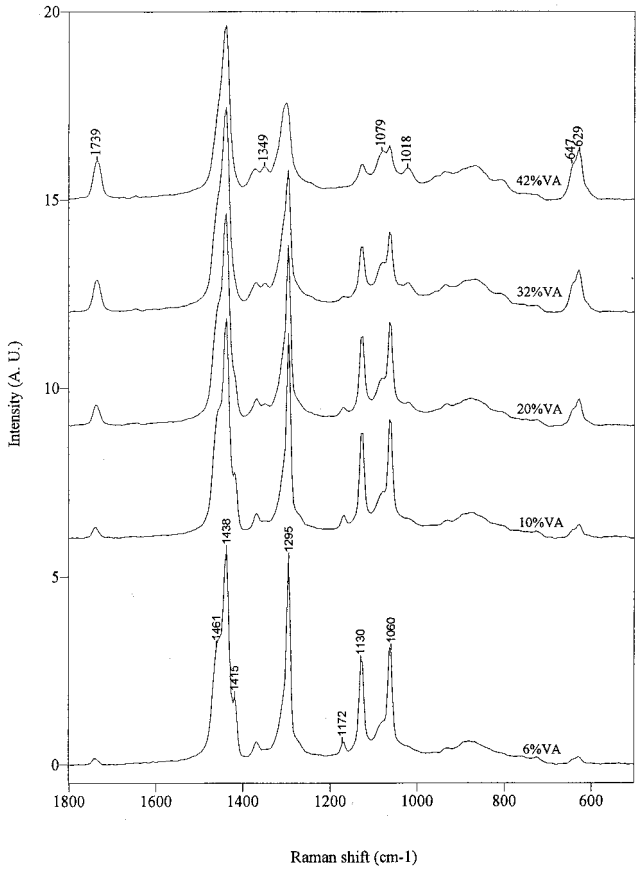

Figure 1. FT-Raman spectra of five representative EVA

discriminated from one another by a score plot of the principal component analysis (PCA). Partial least-squares (PLS) regression was applied to develop calibration models which predict the VA content in EVA.

The FT-Raman spectra of EVA copolymers with VA content ranging from 6 to 42 wt % are presented in Figure 1. The complex changes in the series of spectra of Figure 1 may have been caused by the following factors: (1) compositional change and thus population densities of ethylene and VA contents, (2) configurational and conformational change in the regularity of methylene sequences due to VA inclusion, (3) disruption of the crystalline packing in a unit cell, and (4) redistribution of methylene groups in different phases. It is of both scientific and technological importance to investigate systematically at what stage and in which order these events occur with the increase of VA content in EVA.

In 1978 Strobl an Hagedorn [28] studied the redistribution of phase compositions in EVA with VA increasing from 2.5 to 8.5 wt % using Raman spectroscopy. They proposed a three-phase model for EVA: an orthorhombic crystalline phase, a meltlike amorphous phase, and a disordered phase of anisotropic nature, where chains are stretched but have lost their lateral order. While the previous Raman study was focused on the supramolecular level, the present study assisted by the use of modern fluorescence-free FT-Raman spectroscopy and high-resolution 2D correlation spectroscopy probes the structural changes in EVA copolymers at the molecular and submolecular level.

Experimental Section

Eleven different EVA copolymers with different VA content (6, 7, 8, 10, 15, 20, 25, 26, 28, 32, and 42 wt %) in pellets (approximately 4 mm in diameter) were generously provided by TOSOH Corporation, Tokyo, Japan, and used without further purification. The VA content in EVA was determined by elemental analysis. The crystallinity data (Supporting Information) of these samples were obtained using Strobl and Hagedorn's method.[28]

The NIR-excited FT-Raman spectra of the eleven EVA copolymers were measured at 8 cm^{-1} resolution with a JEOL JRS-FT6500N Raman spectrometer equipped with an InGaAs detector. The excitation source used was the 1064 nm line from a cw Nd:YAG laser (Spectron SL301). The laser power at the sample position was typically 400 mW. Raman scattered light was collected with a 180° backscattering geometry, and all the spectra were the results of the coaddition of 200 interferograms.

For the 2D correlation analysis we used a software named "2D Pocha", which was composed by Daisuke Adachi (Kwansei Gakuin University). The 11 spectra were normalized and divided into four sets according to the VA composition range. Set 1 contains three spectra of copolymers with VA content of 6, 7, and 8 wt %. Set 2 contains three spectra of those with VA content of 10, 15, and 20 wt %. Set 3 contains three spectra of those with VA content of 25, 26, and 28 wt %. Set 4 also contains three spectra of those with VA content of 28, 32, and 42 wt %. The one-dimensional spectra shown at the side and top of the 2D correlation maps are the average over the three spectra of each set of samples. In the 2D correlation maps, regions without dots indicate positive correlation intensities, while regions with dots indicate negative correlation intensities.

Backgrounds

The present 2D FT-Raman correlation spectroscopy study of the structural changes in EVA copolymers is based on the fact that simple composition change alone can give rise to only synchronous correlation peaks but not asynchronous peaks. When VA content is increased by 10 wt %, for example, the ethylene content is certainly reduced by 10 wt %. The synchronous correlation intensity Φ between two bands due to the same comonomer is positive, while that between different comonomers is negative. If the composition change produces strictly proportional change in band intensities, the corresponding asynchronous correlation intensity would be zero. In fact, change in the VA content gives rise to irregular and disproportionate structural changes in EVA, resulting in complex spectral changes. Thus, the appearance of any asynchronous peak in our study should indicate the presence of such structural changes.

The sign of an asynchronous correlation peak $\Psi[\nu_1, \nu_2]$ gives information about the sequential order of intensity changes between two bands at ν_1 and ν_2. According to the rules developed by Noda,[1] $\Phi[\nu_1, \nu_2] < 0$ and $\Psi[\nu_1, \nu_2] > 0$ imply that the intensity change at ν_1 occurs at higher VA content compared to that at ν_2. So do $\Phi[\nu_1, \nu_2] > 0$ and $\Psi[\nu_1, \nu_2] < 0$. $\Phi[\nu_1, \nu_2] < 0$ and $\Psi[\nu_1, \nu_2] < 0$ imply that the intensity change at ν_1 takes place at lower VA content than that at ν_2. So do $\Phi[\nu_1, \nu_2] > 0$ and $\Psi[\nu_1, \nu_2] > 0$. In this paper we shall use these relationships to determine the sequential order of intensity change between two bands.

The nonproportional (nonlinear) nature of composition-induced spectral changes of EVA is also strongly influenced by the average background level of VA content. To accentuate the effect of the background VA level, we subdivided the spectral data into four distinct sets. The 2D correlation spectra of individual data sets are then compared to further elucidate

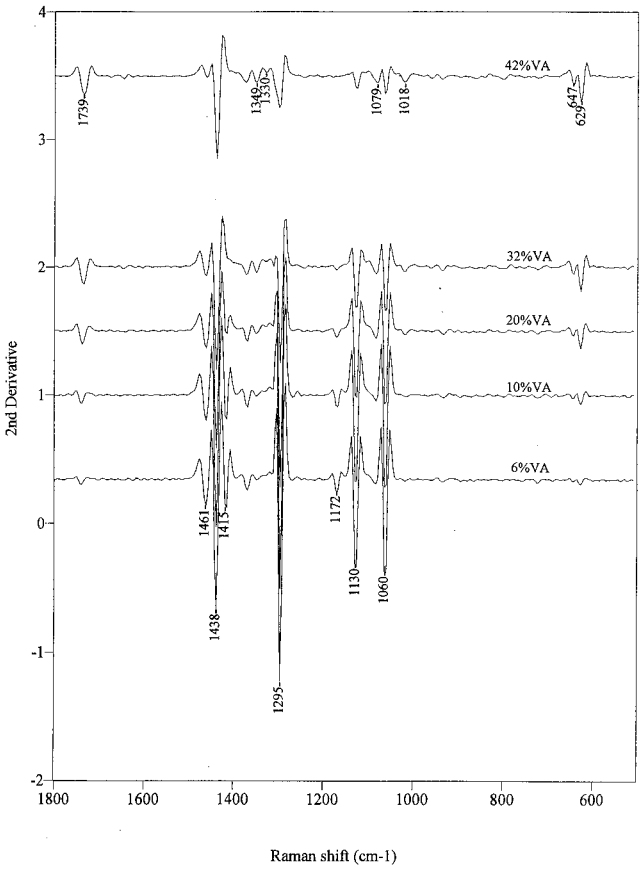

Figure 2. Second derivatives of the FT-Raman spectra of EVA shown in Figure 1

the intricate details of the composition-induced submolecular level reorganization of EVA copolymers under VA content variations.

Results and Discussion

For a detailed assignment of the Raman bands of spectra shown in Figure 1, we present the corresponding second derivatives in Figure 2. Table 1 lists the assignment of the pertinent bands in Figures 1 and 2. The assignment is based on previous studies of crystalline polyethylene [29−32] and partially crystalline polyethylene.[33−35]

1. Set 1. This set contains three EVA copolymers with low VA content of 6−8 wt %. The overall composition change of 2 wt % is relatively small and the spectral changes result mostly from structural changes (phase redistribution, conformation change, etc.) induced by the VA incorporation. Raman bands due to acetate groups will not be considered for this study. 2D correlation of the Raman spectra of set 1 can reflect the characteristic behavior of the low VA level EVA, centered around the composition containing only about 7 wt % VA under 1% perturbation. Figure 3A shows the synchronous correlation spectrum for set 1 in the region of 1500−1200 cm^{-1}. The band at 1415 cm^{-1} arises from the lamellar cores which comprise the orthorhombic crystalline phase, and the band at 1307 cm^{-1} arises from the interlamellar layers which comprise the amorphous phase.[29] In Figure 3A, the cross-peak at (1415, 1307) is negative, indicating that while the intensity of the crystalline band at 1415 cm^{-1} is decreasing, that of the amorphous band at 1307 cm^{-1} is increasing. Thus, with a small increase of VA content in the copolymers of set 1, the crystalline lamellae shrink and the interlamellar amorphous layers expand.

TABLE 1: Assignment of the Bands in Figures 1 and 2

frequency (cm^{-1})	mode	features[a]
629	O−C═O deformation	due to acetate
647	O−C═O deformation	due to acetate
1018	C−C streching of >HC−CH_2	due to vinyl
1060	asymmetric C−C stretching	due to *all-trans*−(CH_2)−$_n$
1079	asymmetric C−C stretching	A (*trans and gauche*)
1110	symmetric C−C stretching	A (*trans and gauche*)
1130	symmetric C−C stretching	due to *all-trans*−(CH_2)−$_n$
1172	CH_2 rocking	C
1295	CH_2 twisting	due to *all-trans*−(CH_2)−$_n$
1307	CH_2 twisting	A
1330	CH_2 wagging	A
1349	CH_2 wagging	A
1373	CH_2 wagging	A
1380	CH_3 symmetric bending	due to acetate
1415	CH_2 bending	C
1430	CH_3 asymmetric bending	due to acetate
1434	CH_2 bending	N
1438	CH_2 bending	C
1446	CH_2 bending	N
1461	2 × CH_2 rocking	due to *all-trans*−(CH_2)−$_n$
1739	C═O stretching	due to acetate

[a] A: amorphous. C: crystalline. N: anisotropic.

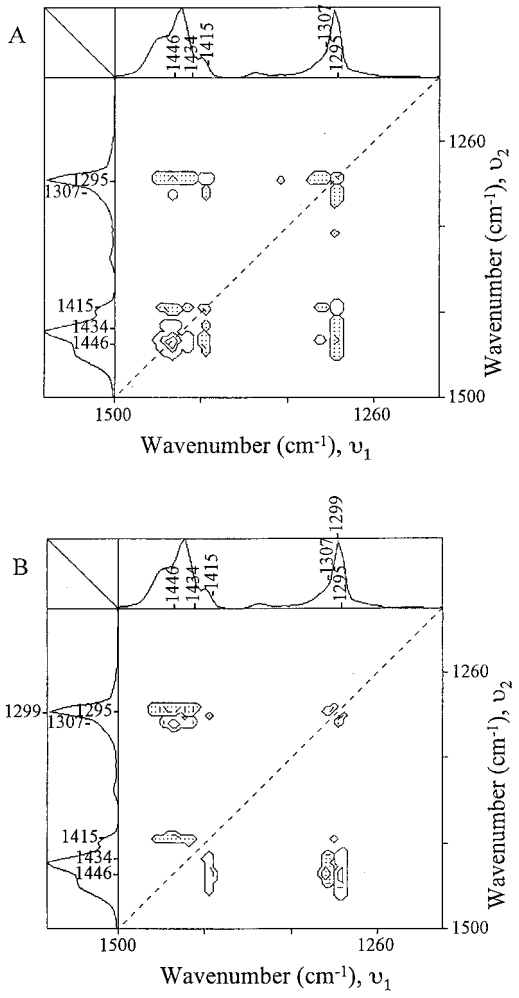

Figure 3. (A) Synchronous 2D FT-Raman correlation spectrum in the region of 1500−1200 cm^{-1} for EVA copolymers with VA from 6 to 8 wt %. (B) The corresponding asynchronous correlation spectrum.

The band at 1415 cm^{-1} appears only for the orthorhombic crystalline packing of methylene chains. [28−35] The unit cell has two methylene segments, each containing 2 × CH_2 groups. The

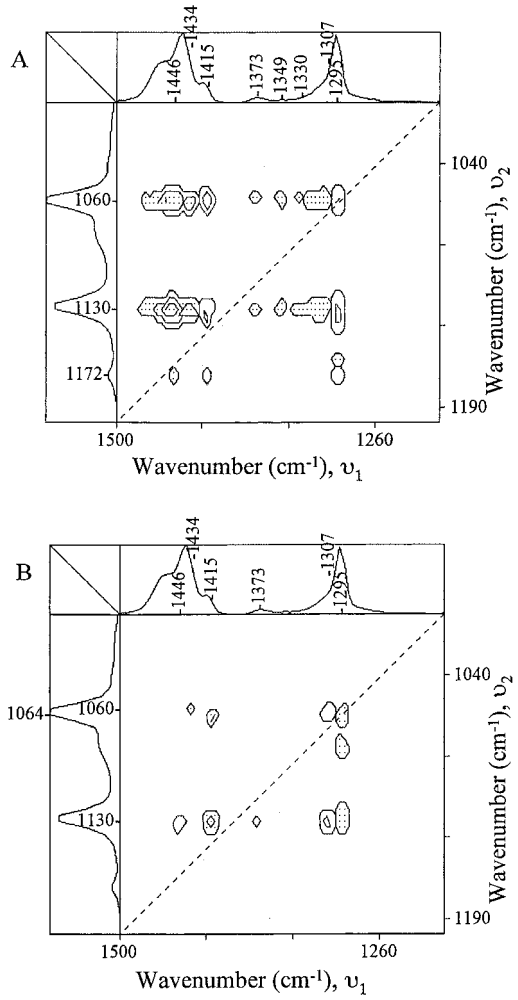

Figure 4. (A) Synchronous 2D FT-Raman correlation spectrum in the region of 1500−1200 cm^{-1} and 1200−1000 cm^{-1} for EVA copolymers with VA from 6 to 8 wt %. (B) The corresponding asynchronous correlation spectrum.

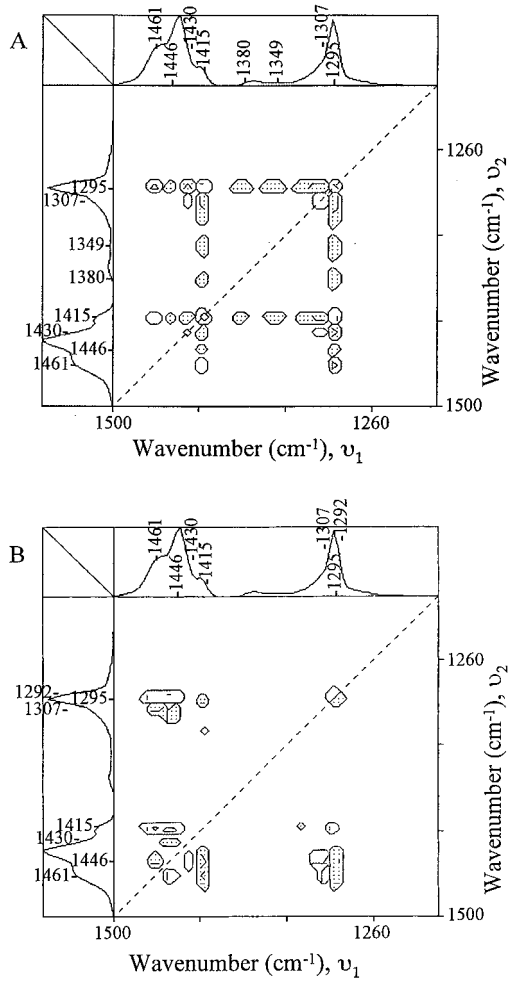

Figure 5. (A) Synchronous 2D FT-Raman correlation spectrum in the region of 1500−1200 cm^{-1} for EVA copolymers with VA from 10 to 20 wt %. (B) The corresponding asynchronous correlation spectrum.

two methylene segments are oriented with their C−C−C planes normal to each other. The CH_2 bending vibration of each segment can occur in-phase or out-of-phase with respect to that of its neighboring segment, thereby producing the correlation splittings of $A_{1G}\delta(CH_2)$ mode at 1415 and 1438 cm^{-1}, respectively. It is noteworthy that the band at 1415 cm^{-1} appears for set 1 in Figures 3A and B, while the crystalline band at 1438 cm^{-1} does not. The crystalline band at 1438 cm^{-1} appears only when VA contents exceed 25 wt % (see Figure 7B). The most obvious explanation is that the in-phase mode at 1415 cm^{-1} can exist only for sufficiently long methylene sequences that contain many 2 × CH_2 (although the requirement for orthorhombic packing is just that the segment contains one 2 × CH_2). The out-of-phase mode at 1438 cm^{-1} can exist even for short segments containing only one 2 × CH_2, bounded by the VA comonomers.

In Figure 3A the bands at 1446 and 1434 cm^{-1} have negative correlation with the crystalline band at 1415 cm^{-1} and positive correlation with each other. The band at 1446 cm^{-1} has positive correlation with the amorphous band at 1307 cm^{-1}. These facts indicate that the intensity change of the bands at 1446 and 1434 cm^{-1} has the same direction as the amorphous band at 1307 cm^{-1} and opposite direction with respect to the crystalline band at 1415 cm^{-1}. However, it is not enough to conclude that they are due to the amorphous phase. In fact, the bands at 1446 and 1434 cm^{-1} have asynchronous relationship with the amorphous band at 1307 cm^{-1}, as shown in Figure 3B. The appearance of any asynchronous peak $\Psi[\nu_1, \nu_2]$ implies that the chemical groups representing the bands at ν_1 and ν_2 are not in the same phase or physical state. Consequently, these bands should arise from an anisotropic phase, where the methylene sequences have *all-trans* conformation and some kind of lateral order, but cannot pack as tightly as those in the crystalline phase. This phase is believed to exist as transition layer between the lamella and the interlamellar amorphous layer.[29] However, this anisotropic layer is not quite like that originally proposed by Strobl and Hagedorn,[28] which has not any lateral order. The acetate side groups act as spacers between adjacent chains and reduce the interaction force between their hydrogen atoms, and hence the magnitude of correlation splittings.[32] The bands at 1446 and 1434 cm^{-1} are thus assigned to the correlation splittings of CH_2 bending vibrations. The splitting here is 8 cm^{-1}, considerably smaller than the 23 cm^{-1} splitting between 1438 and 1415 cm^{-1} in the crystalline phase.

The order of intensity changes between two bands is listed in Table 2. From the first and second rows of Table 2, it is concluded that the intensity variation of the bands at 1446 and 1434 cm^{-1} takes place before that of the band at 1307 cm^{-1}. Thus, for set 1 the inclusion of VA comonomer first causes the expansion of the anisotropic phase, then the expansion of the amorphous phase. The physical implication here is that the acetate side groups act as spacers between adjacent chains, thereby converting the tightly packed orthorhombic phase to

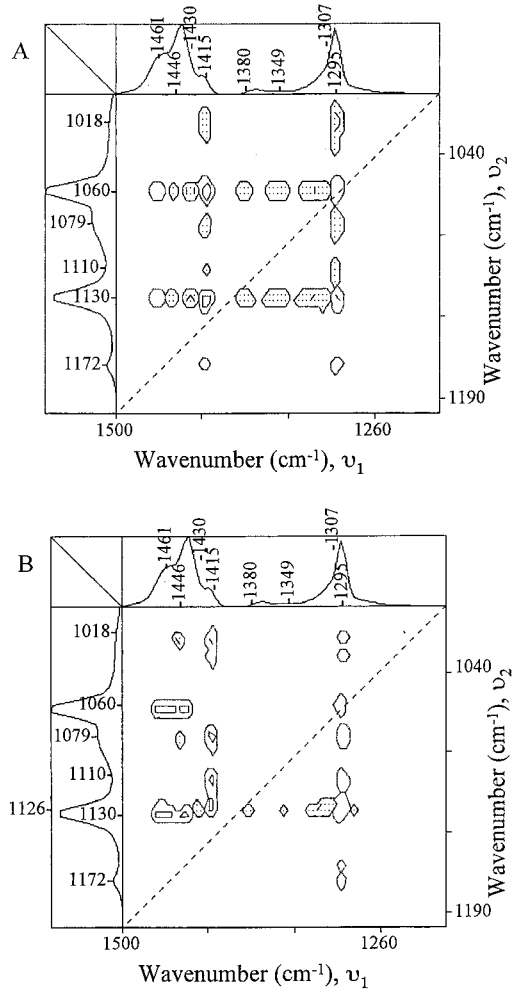

Figure 6. (A) Synchronous 2D FT-Raman correlation spectrum in the region of 1500−1200 cm^{-1} and 1200−1000 cm^{-1} for EVA copolymers with VA from 10 to 20 wt %. (B) The corresponding asynchronous correlation spectrum.

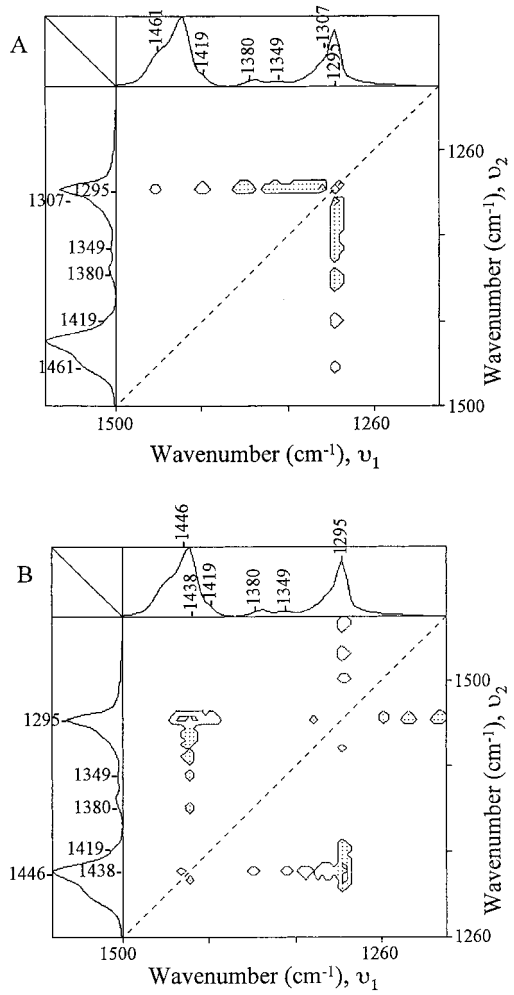

Figure 7. (A) Synchronous 2D FT-Raman correlation spectrum in the region of 1500−1200 cm^{-1} for EVA copolymers with VA from 25 to 28 wt %. (B) The corresponding asynchronous correlation spectrum.

the loosely packed anisotropic phase. The anisotropic phase then transforms to the amorphous phase.

Figure 3B resolves two bands at 1295 and 1299 cm^{-1}. The one-dimensional spectrum in Figure 1 gives only one band around 1295 cm^{-1}, which is well-known as due to the in-phase twisting of methylenes along *all-trans* chains. Both the orthorhombic crystalline phase and the anisotropic phase can contribute to its intensity. The band at 1299 cm^{-1} has asynchronous relationship with the crystalline band at 1415 cm^{-1} (Figure 3B) and must be due to the anisotropic phase. The band at 1295 cm^{-1} has asynchronous relationship with the anisotropic bands at 1446 and 1434 cm^{-1} and must be due to the crystalline phase.

Figure 4A shows the synchronous correlation spectrum for the samples containing 6, 7 and 8 wt % VA in the region 1500−1200 cm^{-1} and 1200−1000 cm^{-1}. The band at 1172 cm^{-1} is known as due to the crystalline phase (Table 1). Thus, its positive correlation with the crystalline band at 1415 cm^{-1} is expected. The bands at 1130 and 1060 cm^{-1} are due to asymmetric and symmetric C−C stretching vibrations, respectively. These bands appear for *all-trans* chains of $CH_3(CH_2)_n$-CH_3 for $n \geq 6$.[37] These bands should be highly overlapped, since they may come from both the anisotropic phase and the orthorhombic crystalline phase.

As shown in Figure 4A, the bands at 1130 and 1060 cm^{-1} have positive synchronous correlation with the crystalline bands at 1415 cm^{-1}, negative correlation with the amorphous band at 1307 cm^{-1}, and negative correlation with the anisotropic bands at 1446 and 1434 cm^{-1}. Therefore, the amount of *all-trans* chains in EVA copolymers is reduced with the increase of VA content. The *all-trans* bands at 1130 and 1060 cm^{-1} have negative correlation with the bands 1373 and 1349 cm^{-1}. The band at 1349 cm^{-1} is due to CH_2 wagging vibration of the *gauche*−*gauche* conformations, and the band at 1373 cm^{-1} comes from CH_2 wagging vibration of the *trans-gauche* conformations.[24] Thus, various *gauche* conformations appear with the incorporation of VA comonomers.

The corresponding asynchronous correlation map (Figure 4B) resolves two bands at 1064 and 1060 cm^{-1}. The band at 1060 cm^{-1} has asynchronous relationship with the anisotropic band at 1434 cm^{-1} and must arise from the crystalline lamellae. The band at 1064 cm^{-1} has asynchronous relationship with the crystalline band at 1415 cm^{-1} and must be due to the anisotropic phase. The third row of Table 2 shows that the intensity change of the amorphous band at 1307 cm^{-1} occurs after that of the band at 1064 cm^{-1}. Thus, the expansion of the interlamellar amorphous layers occurs after that of the anisotropic transition layers with the increase of VA content. This conclusion is consistent with that derived from Figure 3B.

2. Set 2. This set contains three EVA copolymers with somewhat higher VA content of 10, 15, and 20 wt %. The overall composition change of 10 wt % is rather large, and Raman bands due to acetate groups should be considered. 2D

TABLE 2: Synchronous and Asynchronous Correlation Intensities and the Order of Intensity Change between Two Bands[a]

number	Φ	Ψ	order
1	Φ(1446, 1307) > 0	Ψ(1446, 1307) > 0	1446 cm^{-1} before 1307 cm^{-1}
2	Φ(1434, 1307) > 0	Ψ(1434, 1307) > 0	1434 cm^{-1} before 1307 cm^{-1}
3	Φ(1307, 1064)<0	Ψ(1307, 1064) > 0	1307 cm^{-1} after 1064 cm^{-1}
4	Φ(1461, 1415) > 0	Ψ(1461, 1415) > 0	1461 cm^{-1} before 1415 cm^{-1}
5	Φ(1446, 1430) > 0	Ψ(1446, 1430)<0	1446 cm^{-1} after 1430 cm^{-1}
6	Φ(1446, 1079) > 0	Ψ(1446, 1079)<0	1446 cm^{-1} after 1079 cm^{-1}
7	Φ(1430, 1126)<0	Ψ(1430, 1126)<0	1430 cm^{-1} before 1126 cm^{-1}
8	Φ(1380, 1126)<0	Ψ(1380, 1126)<0	1380 cm^{-1} before 1126 cm^{-1}
9	Φ(1438, 1130) > 0	Ψ(1438, 1130) > 0	1438 cm^{-1} before 1130 cm^{-1}
10	Φ(1438, 1060) > 0	Ψ(1438, 1060) > 0	1438 cm^{-1} before 1060 cm^{-1}
11	Φ(1419, 1130) > 0	Ψ(1419, 1130) > 0	1419 cm^{-1} before 1130 cm^{-1}
12	Φ(1419, 1060) > 0	Ψ(1419, 1060) > 0	1419 cm^{-1} before 1060 cm^{-1}
13	Φ(1419, 1295) > 0	Ψ(1419, 1295) > 0	1419 cm^{-1} before 1295 cm^{-1}
14	Φ(1461, 1295) > 0	Ψ(1461, 1295)<0	1461 cm^{-1} after 1295 cm^{-1}
15	Φ(1461, 1130) > 0	Ψ(1461, 1130)<0	1461 cm^{-1} after 1130 cm^{-1}
16	Φ(1461, 1060) > 0	Ψ(1461, 1060)<0	1461 cm^{-1} after 1060 cm^{-1}
17	Φ(1419, 1130) > 0	Ψ(1419, 1130) > 0	1419 cm^{-1} before 1130 cm^{-1}
18	Φ(1419, 1060) > 0	Ψ(1419, 1060) > 0	1419 cm^{-1} before 1060 cm^{-1}

*ν_1 after (before) ν_2 means the intensity change of the band at υ_1 occurs at higher (lower) VA contents than that at υ_2.

correlation of the Raman spectra of set 2 can reflect the behavior of the EVA with low to middle VA content under a large compositional perturbation. Figure 5A shows the synchronous correlation spectrum for set 2 in the region of 1500−1200 cm^{-1}. The band at 1380 cm^{-1} is assigned to the methyl symmetric bending mode of acetate groups. It has negative correlation intensities with the crystalline band at 1415 cm^{-1} and the *all-trans* band at 1295 cm^{-1}, indicating that with the inclusion of VA comonomer the crystallinity of EVA decreases, and the *all-trans* conformers reduce. A band at 1461 cm^{-1} has been assigned to the first overtone of methylene in-phase rocking mode at 730 cm^{-1} by Maxfield et al.,[33] which is characteristic of the $-(CH_2)-_n$ structure for $n \geq 3$.[38] The band at 1461 cm^{-1} has positive synchronous correlation with the crystalline band at 1415 cm^{-1}, implying the shortening of methylene sequences. Moreover, the band at 1461 cm^{-1} has asynchronous relationship with the crystalline band at 1415 cm^{-1} (Figure 5B). The fourth row of Table 2 shows that the event at 1461 cm^{-1} occurs before that at 1415 cm^{-1}, indicating that the shortening of continual methylene sequences takes place ahead of the shrinking of crystalline lamellae as VA content is increased.

A band at 1430 cm^{-1} in Figure 5A is assigned to the CH_3 asymmetric bending mode, in line with the assignment of the band at 1380 cm^{-1} to the CH_3 symmetric bending mode. This assignment is consistent with the fact that the band at 1430 cm^{-1} has positive correlation with the amorphous band at 1307 cm^{-1} and negative correlation with the crystalline band at 1415 cm^{-1}, as shown in Figure 5A. This assignment is also consistent with the asynchronous peak at (1446, 1430 cm^{-1}) in Figure 5B. The fifth row of Table 2 shows that the event at the anisotropic band at 1446 cm^{-1} occurs after the event at 1430 cm^{-1}, indicating that the expansion of the anisotropic transition layers takes place as a result of the incorporation of VA.

Comparing Figures 3B and 5B, it seems that the band at 1299 cm^{-1} moves to 1295 cm^{-1}, while the band at 1295 cm^{-1} shifts to 1292 cm^{-1} for set 2. In other words, the band at 1295 cm^{-1} arises from the anisotropic phase, and the band at 1292 cm^{-1} comes from the crystalline phase of set 2. This conjecture is based on the observation that the band at 1295 cm^{-1} has asynchronous relationship with the crystalline band at 1415 cm^{-1} for set 2. The peak at (1415, 1295 cm^{-1}) is negative in Figure 5B, and it looks like the negative peak at (1415, 1299 cm^{-1}) in Figure 3B. The peak pairs at (1295, 1292 cm^{-1}) and (1292, 1295 cm^{-1}) in Figure 5B look just like the pairs at (1299, 1295 cm^{-1}) and (1295, 1299 cm^{-1}) in Figure 3B. The lower shift of the CH_2 in-phase twisting vibration obviously results from the decrease in n of the $-(CH_2)-_n$ sequences.

Figure 6A shows the synchronous correlation spectrum for set 2 in the region of 1500−1200 cm^{-1} and 1200−1000 cm^{-1}. Three bands at 1018, 1079, and 1110 cm^{-1} first appear for this set of EVA. The band at 1079 cm^{-1} is known as due to the asymmetric C−C stretching vibration of *trans-gauche* alternating $-(CH_2)-_n$ sequences and is often used to estimate the amorphous content in partially crystalline polyethylene.[33,34] The negative peak at (1415, 1079 cm^{-1}) indicates the expansion of the amorphous phase and the shrinking of the crystalline phase. The negative peak at (1295, 1079 cm^{-1}) implies the increase of *trans-gauche* sequences and the reduction of *all-trans* sequences. The band at 1079 cm^{-1} has asynchronous relationship with the crystalline band at 1415 cm^{-1} and the anisotropic band at 1446 cm^{-1}, as shown in Figure 6B, consistent with the fact that it comes from the amorphous interlamellar layers. The sixth row of Table 2 shows that the event at 1446 cm^{-1} takes place after that at 1079 cm^{-1}, indicating that the expansion of the anisotropic transition layers occurs after that of the amorphous phase, as VA content is increased. Interestingly, this sequence of occurrence is opposite to that of set 1. Thus, for a larger level VA incorporation, the expansion of the amorphous phase is caused directly by the composition change.

The bands at 1018 and 1110 cm^{-1} should arise from the amorphous phase, according to their negative synchronous correlation with the crystalline band at 1415 cm^{-1} and the *all-trans* band at 1295 cm^{-1}. The band at 1110 cm^{-1} may be the symmetric counterpart of the asymmetric C−C stretching band at 1079 cm^{-1}. The band at 1018 cm^{-1} may be assigned to the C−C stretching involving >CH−CH_2− groups.

Figure 6B resolves two close bands at 1130 and 1126 cm^{-1}, both due to *all-trans* methylene chains. The band at 1126 cm^{-1} comes from the anisotropic phase, since it has asynchronous relationship with the crystalline band at 1415 cm^{-1}, as well as with the methyl bands at 1430 and 1380 cm^{-1}. The seventh and eighth rows of Table 2 show that the event at 1430 and 1380 cm^{-1} occurs before that at 1126 cm^{-1}, implying that the incorporation of VA groups as spacers gives rise to the expansion of the anisotropic phase. The band at 1130 cm^{-1} is then assigned to the crystalline phase.

3. Set 3. This set contains three EVA copolymers with much higher VA content of 25, 26, and 28 wt %. The overall composition change of the 3 wt % sample is rather small, so that VA bands will not be considered except the methyl band at 1380 cm^{-1}. 2D correlation of the Raman spectra of set 3 can

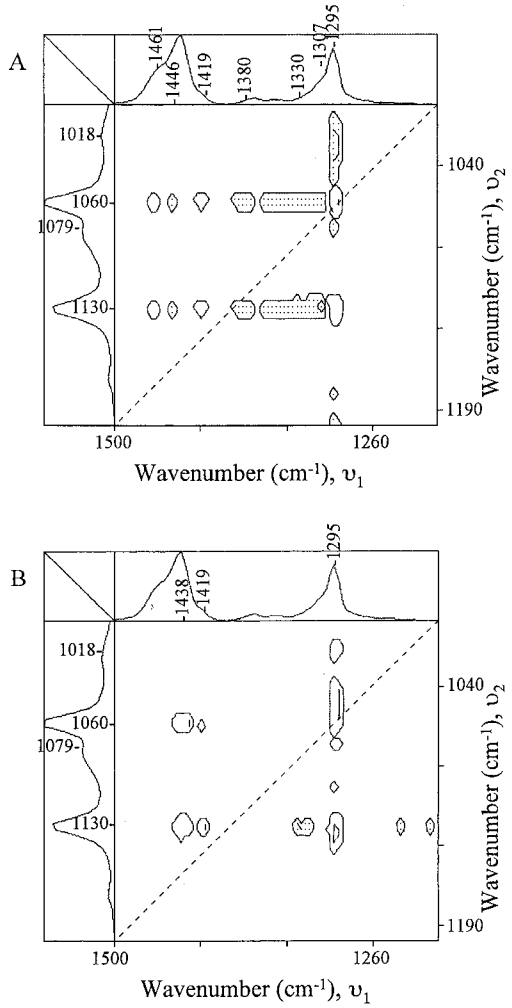

Figure 8. (A) Synchronous 2D FT-Raman correlation spectrum in the region of 1500−1200 cm^{-1} and 1200−1000 cm^{-1} for EVA copolymers with VA from 25 to 28 wt %. (B) The corresponding asynchronous correlation spectrum.

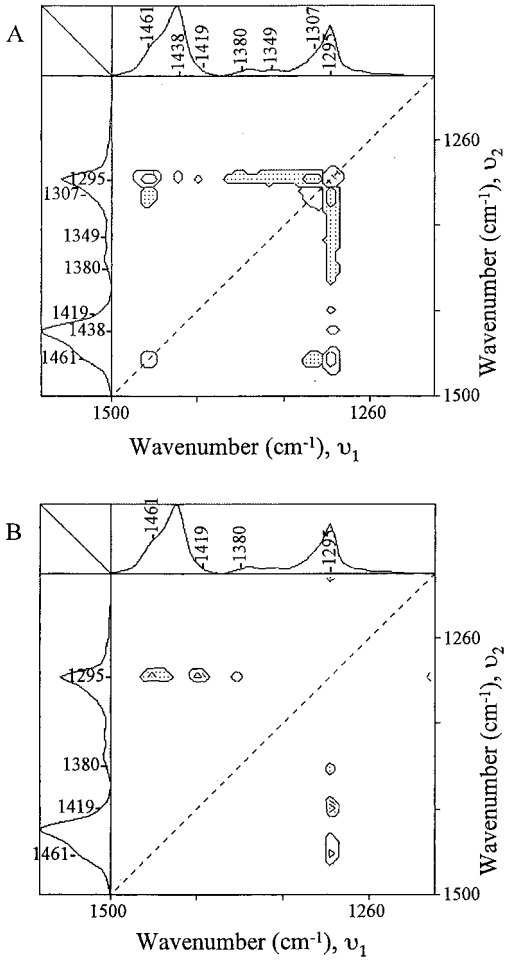

Figure 9. (A) Synchronous 2D FT-Raman correlation spectrum in the region of 1500−1200 cm^{-1} for EVA copolymers with VA from 28 to 42 wt %. (B) The corresponding asynchronous correlation spectrum.

reflect the characteristic behavior of the middle VA level EVA under relatively small addition of VA comonomers. Figure 7A shows the synchronous correlation spectrum for set 3 in the region of 1500−1200 cm^{-1}. All cross-peaks are about the band at 1295 cm^{-1}, indicating that the disappearance of long trans conformers is the most important event. This means that, for VA contents around 26 wt %, the length of continual $-(CH_2)-_n$ segments is approaching the limit for the existence of the long-*trans* band at 1295 cm^{-1}. It was reported that the Raman intensity of the CH_2 in-phase twisting band around 1295 cm^{-1} decreases with the reduction in n.[38] The signs of the cross-peaks at (1461, 1295 cm^{-1}), (1419, 1295 cm^{-1}), (1380, 1295 cm^{-1}), (1349, 1295 cm^{-1}) and (1307, 1295 cm^{-1}) all indicate that long *trans* conformers gradually disappear with the addition of VA comonomers and that *gauche* conformers appear.

The band at 1419 cm^{-1} takes place of the band at 1415 cm^{-1} when VA contents exceed 25 wt %, as seen by comparing Figures 7−10 with Figures 3−6. The frequency shift implies that the correlation splitting of the $A_{1G}\delta(CH_2)$ mode depends on the length of continual $-(CH_2)-_n$ segments, although orthorhombic packing requires only 2 × CH_2 groups in the unit cell. With the decrease of *n*, the correlation splitting decreases.

The corresponding asynchronous correlation spectrum (Figure 7B) is dominated by the event at 1438 cm^{-1}. It is assigned to the out-of-phase counterpart of the band at 1415 cm^{-1}, as stated above. This assignment is consistent with the fact that it has an asynchronous relationship with the *gauche*−*gauche* band at 1349 cm^{-1} and the anisotropic band at 1446 cm^{-1}.

Figure 8A shows the synchronous correlation spectrum in the region of 1500−1200 cm^{-1} and 1200−1000 cm^{-1}. It is seen that the *trans*−*gauche* band at 1079 cm^{-1} has negative synchronous correlation with the *all-trans* band at 1295 cm^{-1} and that the *all-trans* bands at 1130 and 1060 cm^{-1} have negative synchronous correlation with the methyl band at 1380 cm^{-1} and the gauche band at 1307 cm^{-1}. All these cross-peaks give consistent conclusion that the *gauche* conformers grow and the *all-trans* conformers reduce with the increase of VA contents.

The corresponding asynchronous correlation map is shown in Figure 8B. The crystalline band pair at 1438 and 1419 cm^{-1} have asynchronous relationship with the C−C stretching band pair at 1130 and 1060 cm^{-1}. The 9th to 12th rows of Table 2 show that the event at 1438 and 1419 cm^{-1} occurs before that at 1130 and 1060 cm^{-1}. Physically, this means that the orthorhombic packing in the unit cell deforms first, then the 2 × CH_2 segment loses its *all-trans* configuration.

4. Set 4. This set contains three EVA copolymers with very high VA content of 28, 32, and 42 wt %. The overall composition change of 14 wt % is large, and Raman bands resulting from the presence of acetate groups should be considered. 2D correlation of the Raman spectra of set 4 can reveal the behavior of nearly amorphous EVA under large-scale addition of VA comonomers. The crystalline band at 1419 cm^{-1} in the one-dimensional reference spectrum is hardly discernible.

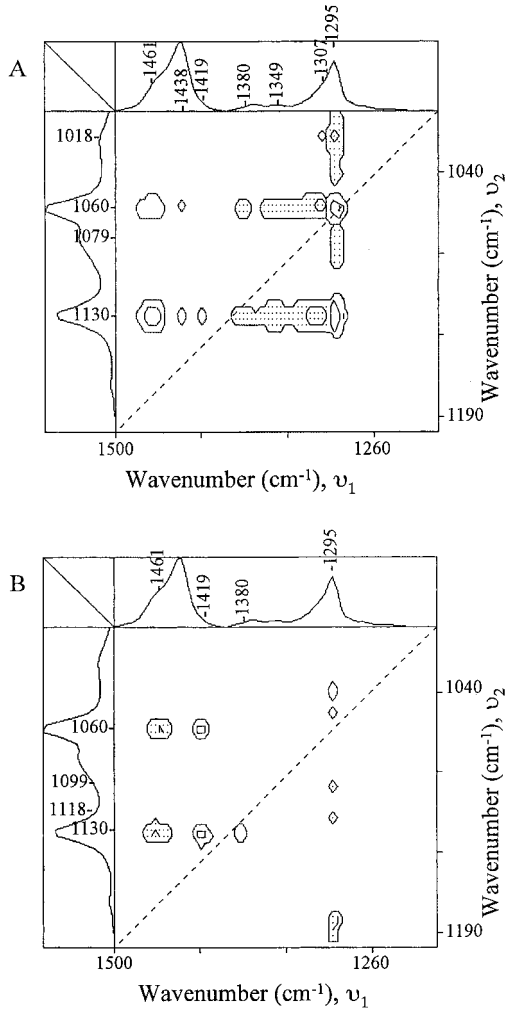

Figure 10. (A) Synchronous 2D FT-Raman correlation spectrum in the region of 1500−1200 cm^{-1} and 1200−1000 cm^{-1} for EVA copolymers with VA from 28 to 42 wt %. (B) The corresponding asynchronous correlation spectrum.

It is noteworthy that the bands at 1446 and 1434 cm^{-1}, characteristic of the anisotropic phase of sets 1−3, do not appear for set 4 throughout the Figures 9A,B and 10A,B. We propose that the anisotropic phase has lost its lateral order when VA contents exceed 28 wt %. Figure 9A shows the synchronous correlation spectrum for set 4 in the region of 1500−1200 cm^{-1}. The band at 1438 cm^{-1} has a positive correlation with the *all-trans* band at 1295 cm^{-1}, consistent with our assignment that it is due to the crystalline phase. Other cross-peaks in Figure 9A have the same implications as those in Figure 7A for set 3.

The corresponding asynchronous correlation spectrum is shown in Figure 9B. The order of intensity variation represented by the cross-peaks is listed in Table 2. The 13th row of Table 2 shows that the event at 1419 cm^{-1} occurs before that at 1295 cm^{-1}. The physical implication is that the deformation of the orthorhombic unit cell takes place first, then the 2 × CH_2 segment loses its *all-trans* conformation. The 14th row of Table 2 shows that the event at 1461 cm^{-1} takes place after that at 1295 cm^{-1}. Both bands are due to methylene deformation modes of *all-trans* $-(CH_2)-_n$ structures. The *n* value for the band at 1295 cm^{-1} must be larger than that for the band at 1461 cm^{-1}, which is known to be 3.[38]

The synchronous correlation map (Figure 10A) in the region of 1500−1200 cm^{-1} and 1200−1000 cm^{-1} looks like that of set 3 in Figure 8A, except the appearance of the crystalline band at 1438 cm^{-1} and the disappearance of the anisotropic band at 1446 cm^{-1}. The corresponding asynchronous correlation spectrum is shown in Figure 10B. The 15th and 16th rows of Table 2 show that the event at 1461 cm^{-1} occurs after that at 1130 and 1060 cm^{-1} due to longer *all-trans* methylene segments. Here, the physical meaning is the same as that derived from the 14th row. The 17th and 18th rows of Table 2 give the same physical implication as that from 11th and 12th rows for set 3.

Conclusion

The present 2D FT-Raman correlation spectroscopy study of composition-dependent spectral variations of eleven EVA copolymers with VA content ranging from 6 to 42 wt % has revealed in detail the composition-induced structural changes in the copolymers. 2D correlation analysis of the spectra of the eleven samples divided into four sets enables us to elucidate the band assignment and the structural changes for each set. For the entire composition change of EVA, the increase of VA contents always causes the crystalline lamellae to shrink, the amorphous interlamellar layers to expand, the *all-trans* $-(CH_2)-_n$ conformers to decrease and the gauche conformers to increase in number. Moreover, the following is concluded for individual set of EVA.

(1) Set 1 with Low-Level VA Contents from 6 to 8 wt %. 2D correlation of this set reflects the characteristic behavior of the EVA containing a relatively low level (7 wt %) of VA under small addition of VA comonomers. An anisotropic phase with *all-trans* methylene segments packing in some lateral order exists, giving rise to the correlation splittings at 1446 and 1434 cm^{-1}. The *all-trans* bands at 1299 and 1064 cm^{-1} are unique to this phase, in contrast to those at 1295 and 1060 cm^{-1} that are characteristic of the orthorhombic crystalline phase. Small addition of VA contents acts as spacers between adjacent chains and converts the orthorhombic unit cell to the anisotropic unit cell. The anisotropic phase then transforms into the amorphous phase.

(2) EVA with Low to Medium Level VA contents from 10 to 20 wt %. 2D correlation of this set reveals the behavior of EVA under large scale VA incorporation. As observed in set 1, the incorporation of VA comonomers as spacers also causes the expansion of the anisotropic phase. Unlike set 1 however, the comonomer content change alone causes the expansion of the amorphous phase. The shortening of continuous methylene sequences results in the lower shift of the CH_2 in-phase twisting vibration mode around 1295 cm^{-1}. The symmetric C−C stretching vibration band at 1126 cm^{-1} is unique to the anisotropic phase of set 2.

(3) EVA with Middle-Level VA Content from 25 to 28 wt %. 2D correlation of this set reflects the characteristic behavior of the middle composition range copolymer under small addition of VA comonomers. The main event is the shortening of *all-trans* methylene sequences, which reduces the correlation splittings of the crystalline phase. The orthorhombic band at 1415 cm^{-1} shifts to 1419 cm^{-1}. The crystalline packing in the unit cell deforms first, then the methylene segment in the unit cell loses its *all-trans* conformation.

(4) EVA with High-Level VA Content from 28 to 42 wt %. 2D correlation of this set reveals the behavior of predominantly amorphous EVA under large-scale addition of VA comonomers. The main event is the further shortening of *all-trans* CH_2 sequences, resulting in the deformation of the orthorhombic unit cell and the decrease of the crystalline band at 1438 cm^{-1}. The anisotropic phase loses its lateral order for set 4.

Acknowledgment. The authors thank the TOSOH Corp., Tokyo, Japan, for providing the EVA samples. This work was supported by a Grant-in-Aid to Y. Ozaki (Grant 09640616) from the Ministry of Education, Science, and Culture, Japan.

Supporting Information Available: Table of the crystallinity parameters of 11 EVA copolymers. This material is available free of charge via the Internet at http://pubs.acs.org.

References and Notes

(1) Noda, I. *Appl. Spectrosc*. **1993,** *47*, 1329.
(2) Noda, I. *Bull. Am. Phys. Soc*. **1986**, *31*, 520.
(3) Noda, I. *J. Am. Chem. Soc.* **1989**, *111*, 8116.
(4) Noda, I. *Appl. Spectrosc*. **1990,** *44*, 550.
(5) Ozaki, Y.; Noda, I. *J. NIR Spectrosc.* **1996**, *4*, 85.
(6) Gustafson, T.; et al. In *Time-Resolved Vibrational Spectroscopy V*; Lau, A., Siebert, F., Eds.; Springer-Verlag: Berlin, 1994; pp131−135.
(7) Noda, I.; Liu, Y.; Ozaki, Y.; Czarnecki, M. A. *J. Phys. Chem*. **1995**, *99*, 3068.
(8) Sefara, N. L.; Magtoto, N. P.; Richardson, H. H. *Appl. Spectrosc*. **1997,** *51*, 536.
(9) Czarnecki, M. A.; Wu, P.; Siesler, H. W. *Chem. Phys. Lett*. **1998**, *283*, 326.
(10) Nabet, A.; Pezolet, M. *Appl. Spectrosc*. **1997,** *51*, 466.
(11) Liu, Y.; Ozaki, Y.; Noda, I. *J. Phys. Chem*. **1996**, *100*, 7327.
(12) Noda, I.; Liu, Y.; Ozaki, Y. *J. Phys. Chem*. **1996**, *100*, 8665.
(13) Ozaki, Y.; Liu, Y.; Noda, I. *Macromolecules* **1997**, *30*, 2391.
(14) Müller, M.; Buchet, R.; Fringeli, U. P. *J. Phys. Chem*. **1996**, *100*, 10810.
(15) Czarnecki, M. A.; Maeda, H.; Y. Ozaki; Suzuki, M.; Iwahashi, M. *J. Phys. Chem. A* **1998**, *102*, 9117.
(16) Wang, Y.; Murayama, K.; Myojo, Y.; Tsenkova, R.; Hayashi, N.; Ozaki, Y. *J. Phys. Chem. B* **1998**, *102*, 6655.
(17) Ren, Y.; Shimoyama, M.; Ninomiya, T.; Matsukawa, K.; Inoue, H.; Noda, I.; Ozaki, Y. (*Appl. Spectrosc.* **1999**. In press.
(18) Noda, I.; Liu, Y.; Ozaki, Y. *J. Phys. Chem*. **1996**, *100*, 8674.
(19) Schultz, C. P.; Fabian, H.; Mantsch, H. H. *Biospectroscopy* **1998**, *4*, 19.
(20) Ren, Y.; Ozaki. Y.; Murakami, T.; Nishioka, T.; Nakashima, K.; Noda, I. *Macromolecules* **1999**. In press.
(21) Hendra, P. J.; Johes, C. H.; Warnes, G. *Fourier transform Raman Spectroscopy*, *Instrumentation and Chemical Applications;* Ellis Horwood: Chichester, 1991.
(22) Schrader, B. In *practical Fourier Transform Infrared Spectroscopy;* Ferraro, J. R., Krishnan, K., Eds.; Academic Press: San Diego, 1990.
(23) Fawcett, A. H. *Polymer Spectroscopy;* John Wiley & Sons: Chichester, 1996.
(24) Utracki, L. A. *Polymer Alloys and Blends, Thermodynamics and Rheology;* Carl Hanser: Munich, 1989.
(25) Doak, K. W. *Encyclopedia of Polymer Science and Engineering;* John Wiley and Sons: New York, 1985; Vol. 6, p 421
(26) Dumcan, R. E. In *Modern Plastics Encyclopedia*; Agranoff, J., Ed.; McGraw-Hill: New York, 1988; p 57.
(27) Shimoyama, M.; Maeda, H.; Matsukawa, K.; Inoue, H.; Ninomiya, T.; Ozaki, Y. *Vib. Spectrosc.* **1997**, *14*, 253.
(28) Strobl, G. R.; Hagedorn, W. *J. Polym. Sci.: Polym. Phys. Ed.* **1978**, *16*, 1181.
(29) Hendra, P. J.; Agbenyega, J. K. *The Raman Spectra of Polymers*; John Wiley & Sons: Chichester, 1993; sections D_1 and E_2.
(30) Bentley, P. A.; Hendra, P. J. *Spectrochim. Acta, Part A* **1995,** *51*, 2125.
(31) Gall, M. J.; Hendra, P. J.; Peacock, C. J.; Cudby, M. E. A.; Willis, H. A. *Spectrochim. Acta, Part A* **1972,** *28*, 1485.
(32) Boerio, F. J.; Koenig, J. L. *J. Chem. Phys.* **1970**, *52*, 3425.
(33) Maxfield, J.; Stein, R. S.; Chen, M. C. *J. Polym. Sci.: Polym. Phys. Ed.* **1978,** *16*, 37.
(34) Glotin, M.; Domszy, R.; Mandelkern, L. *J. Polym. Sci.: Polym. Phys. Ed.* **1983,** *21*, 285.
(35) Tarazona, A.; Koglin, E.; Coussens, B. B.; Meier, R. J. *Vib. Spectrosc.* **1997**, *14*, 159.
(36) Lippert, J. L.; Peticolas, W. L. *Proc. Natl. Acad. Sci. U.S.A.* **1971**, *68*, 1572.
(37) Koenig, J. L. *Spectroscopy of Polymers*; American Chemical Society: Washington, DC, 1992; p 105 about the vibrational spectra of polyethylene and p 89 about the *trans* and *gauche* conformation of polyethylene.
(38) Lin-Vien, D.; Colthup, N. B.; Fateley, W. G.; Grasselli, J. G. *Infrared and Raman Characteristic Frequencies of Organic Molecules*; Academic Press Inc.: San Diego, 1991; p 15.